

PAPER • OPEN ACCESS

Mitigation of irregular burning in a small solid propellant rocket motor

To cite this article: M Elkshen *et al* 2020 *IOP Conf. Ser.: Mater. Sci. Eng.* **973** 012002

View the [article online](#) for updates and enhancements.

You may also like

- [Electric propulsion for satellites and spacecraft: established technologies and novel approaches](#)
Stéphane Mazouffre
- [Nanoparticles for solid rocket propulsion](#)
L Galfetti, L T De Luca, F Severini et al.
- [Study on Main curvature of Stress Relaxation Modulus of a Double-base solid propellant](#)
Zhang Jian-bin, Guo Lei, Li Guang-hua et al.



The Electrochemical Society
Advancing solid state & electrochemical science & technology

243rd Meeting with SOFC-XVIII

Boston, MA • May 28 – June 2, 2023

Accelerate scientific discovery!

Learn More & Register



Mitigation of irregular burning in a small solid propellant rocket motor

M E Ikshen¹, H Belal² and M A Al-Sanabawy³

¹M.Sc. Student, Rocket Department, Military Technical College, Egypt

²Assistant Professor, Rocket Department, Military Technical College, Egypt

³Associate Professor. Rocket Department, Military Technical College, Egypt
hbelal@mtc.edu.eg

Abstract. An irregular burning phenomenon arises in some solid propellant motors (SRM), where the time-averaged pressure differs largely from that dedicated by instantaneous area burning. This phenomenon is generally considered the result of the interaction of pressure disturbances within the motor cavity with solid propellant deflagration. Hence, it is a combustion-dependent acoustic phenomenon. Historically, different suppression devices included the classical resonance rods and paddles, and arrays of acoustic resonators and various baffle arrangements were applied. In this paper, irregular burning which arises in a modification of a shoulder-launched rocket is investigated. Several techniques dealing with the irregular burning problem were attempted. In each case, the signal of pressure was analysed in the time domain through time average and AC pressure signal, and in the frequency domain through Fourier transform and power spectral density. The most successful technique was the drilling of holes through the grain, connecting the perforation to the external burning region of the cylinder. Next was the increasing of blocking factor, both methods lead to stabilizing the modified motor.

1. Introduction

Combustion instability has plagued SRM development for many years. Its occurrence has produced events ranging from unsatisfactory ballistic performance to tolerated pressure oscillations [1]. Irregular burning may be considered one of the exhibitions of combustion instability, in which the pressure varies from the predicted pressure trace dedicated by a balance of mass-generated from burning and mass discharged from the nozzle and still not oscillatory [2]. Usually, irregular burning is accompanied by a DC shift in pressure above or below the natural values.

In general, unstable burning in a solid propellant rocket motor is characterized by undesirable irregularities in the combustion pressure and the linear burning rate. Figure 1, presents the terminology pertinent to the different types of burning that have been observed together with brief descriptions of the principal phenomena associated with the principal types of unstable burning. The frequencies of such oscillations correspond to one or more of the acoustical modes relevant to the geometry of the cavity wherein the combustion arises, hence the term resonant burning. Figure 1 illustrates the pressure-time curves for the different types of burning.



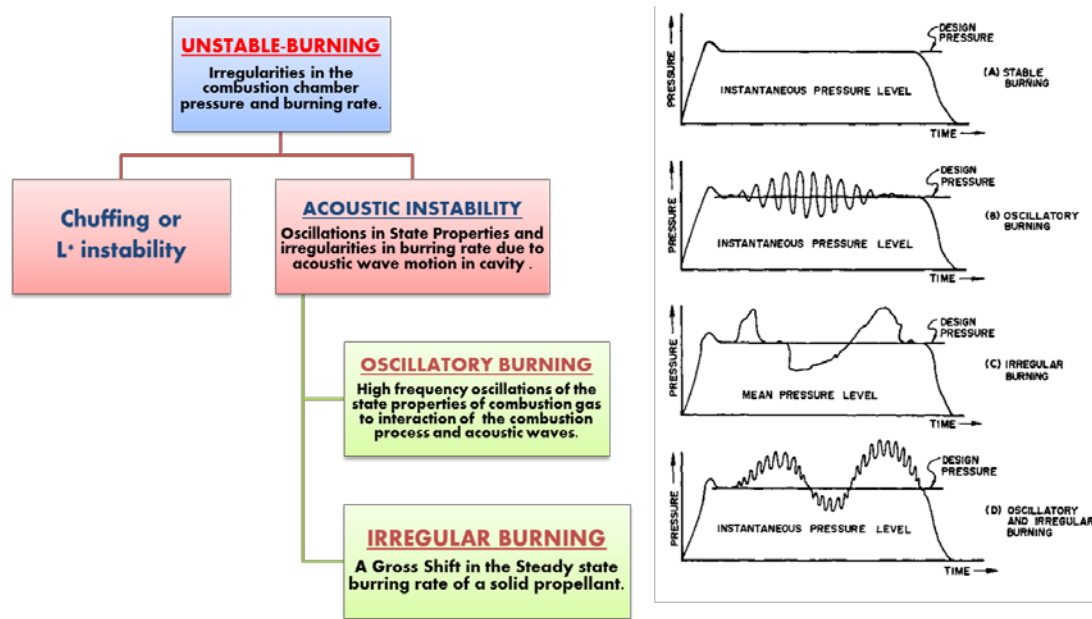


Figure 1. Unstable burning in a solid rocket motor[3].

Generally, the disturbances initially occur at a very small amplitude. If this state continued, combustion instability would be far less troublesome. However, the dynamic response of the combustion response to fluctuations in the internal flow field can result in the amplification of the initial disturbance and is often accompanied by a significant rise in base chamber pressure, called a DC pressure shift and limiting amplitudes of the oscillations[4],[5]. This occurs when the oscillatory gas motion is accompanied by a shift in the mean chamber pressure. In addition to fluctuating motor performance, a significant DC shift in chamber pressure may menace the structural integrity and possibly lead to explosive failure of the motor case[6]–[8].

Historically, several techniques for dealing with the irregular burning problem were attempted. The best success of these techniques was radial holes, in which holes are drilled radially across the web of tubular grains, connecting the perforation to the external burning region of the cylinder. However, drilling toward the head end has been observed to be much more effective in eliminating secondary peaks than drilling the grain near the nozzle end. The stabilization which is obtained by drilling powder grains can also be accomplished by insertion of rods into the inner channel. Here also the effect on pitting of the inner surface of the grain is observed to be local, with head-end stabilization more important, than nozzle end stabilization in eliminating pressure peaks[9],[10].

The term "nozzle damping" represents the amount of the acoustic energy that is convected out of the combustion chamber through the nozzle. Factors such as the nozzle throat size relative to the time-varying chamber port area, the throat erosion rate and how much the throat is submerged in the chamber have a major effect on this term. Additionally, nozzle damping is the largest factor for axial modes and is small for tangential and radial modes[11]–[13].

These techniques were supposed to affect the geometry of oscillating gas volume to change (usually increase) the frequencies and structure of the ordinary modes, thereby placing them outside the range in which the propellant will drive most strongly. Changes in the mode shapes relative to the distribution of burning surface may be such as to reduce the driving of combustion processes[14].

In this paper, a modification of a shoulder-launched rocket was attempted. The modification necessitated a change from forward multi-nozzle into a single central-nozzle keeping all other parameters unaltered. However, an irregular burning phenomenon emerged. This research attempts to mitigate these irregularities by applying different techniques in order to gain a better understanding of the phenomenon and its suppression methods.

2. The Motor

The original motor with 6 forward annular nozzles is shown in figure 2. Isometric views of the nozzle are shown in figure 3. In figure 4, the modified motor with central-nozzle is shown. The propellant used is a double-base propellant with the detailed composition given in table 1. The propellant grain was tubular without inhibited end.

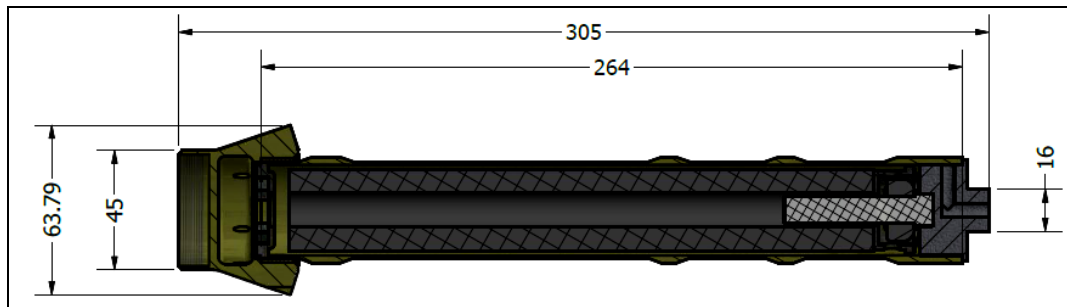


Figure 2. Test motor with multi-nozzle.

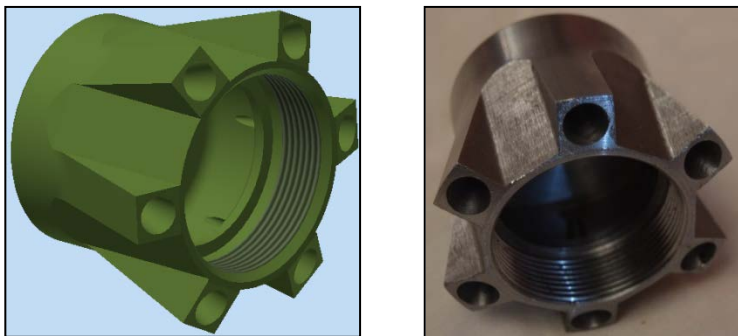


Figure 3. Multi-nozzle



Figure 4. Test motor with central-nozzle.

Table 1. Composition of the double-base propellant.

Propellant	Density (g/cm ³)	Weight (g)
NC	1.653	59.0
NG	1.6	31.0
EC	1.14	5.0
C ₁₆ H ₂₂ O ₄	1.05	2.0
C ₇ H ₆ N ₂ O ₄	1.52	3.0
PBN ₂ O ₆	4.53	2.0
C	2.26	.30

3. The problem

The static test for the original motor is shown in figure 5. The results show a typical pressure-time curve, without any instability or fluctuation in pressure. It is clear that the pressure-time trace has no oscillations except at ignition and burnout.

The problem arises when replacing the multi-nozzle with a single central nozzle in the same motor, keeping the same throat area and using the same propellant grain. The modified motor shows a different pressure-time trace in static tests. The pressure-time trace (P-t trace) shows irregular burning phenomena, and where the pressure varies from the value predicted using the instantaneous burning area.

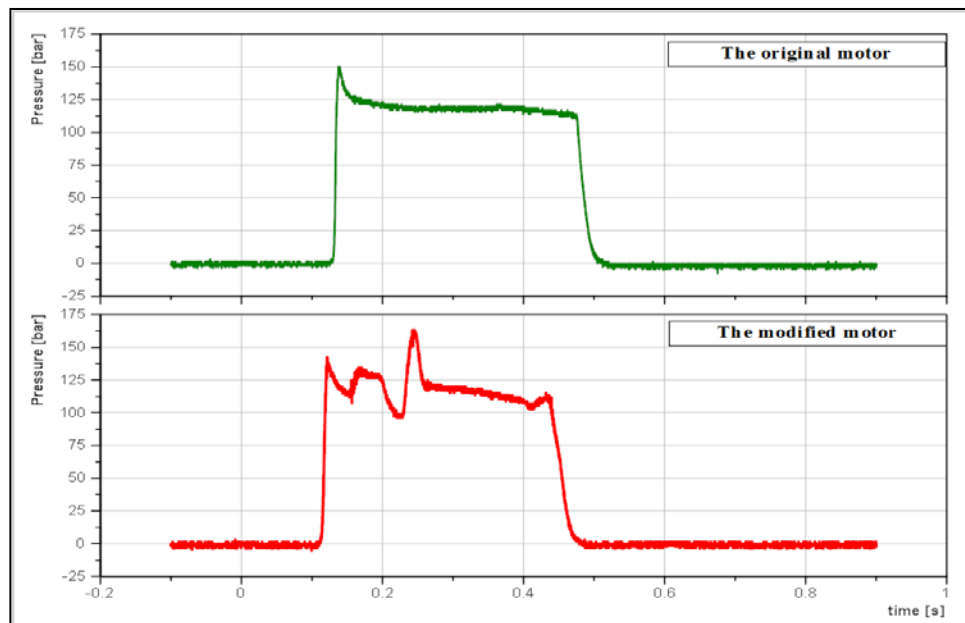


Figure 5. The (P-t) trace for the original motor and the modified motor.

4. Experimental technique and test matrix arrangement

Different methods are attempted to suppress the irregular burning: (a) using resonance rod, figure 6, (b) drilled holes[15], figure 7, and (c) nozzle admittance (damping) changes through using nozzles with different diameters[16]–[21].

The stabilizing effect of a hole is slightly decreased if the diameter of the hole is made very small in comparison with that of the axial perforation. However, increasing the diameter of the radial hole further than 0.4 times that of the axial perforation does not add to the stabilizing effect. So, the chosen diameter was 4 mm, (0.4 times the axial perforation). The burning area slightly increases but has no effect on the ballistic performance of the motor [15], figure 8.

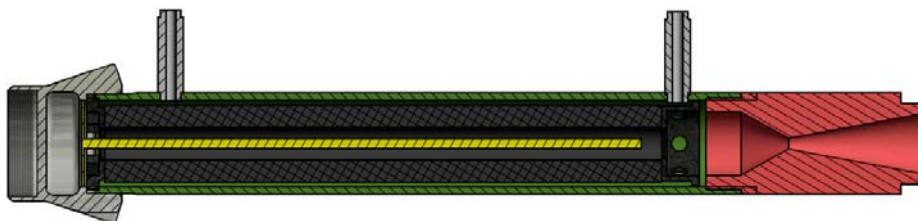


Figure 6. Test motor with resonance rod.

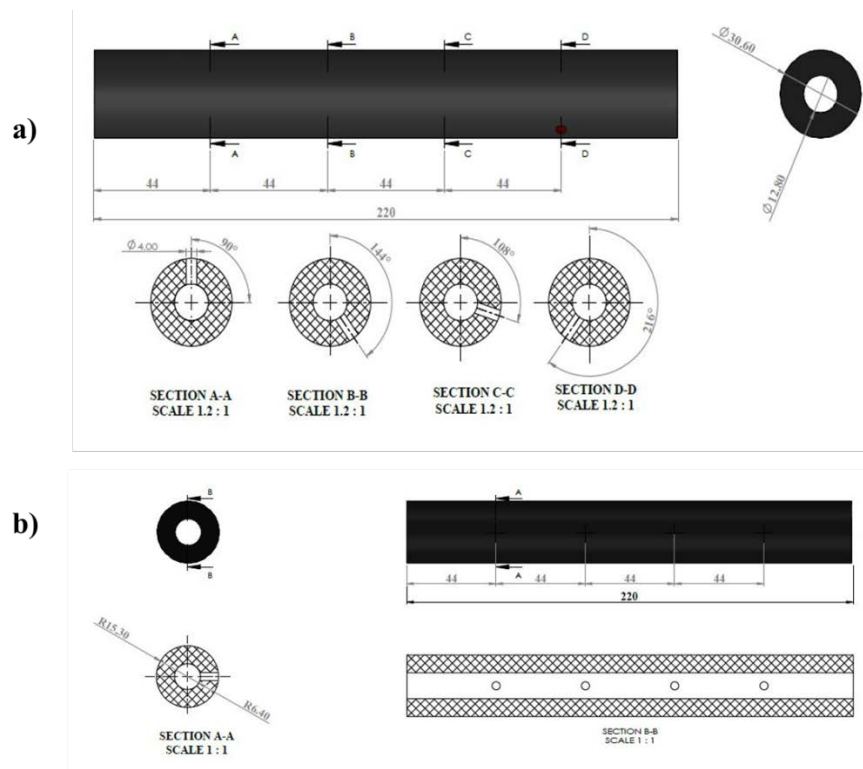


Figure 7. The double-base grain with (a) 4 radial holes (b) 4 inline holes.

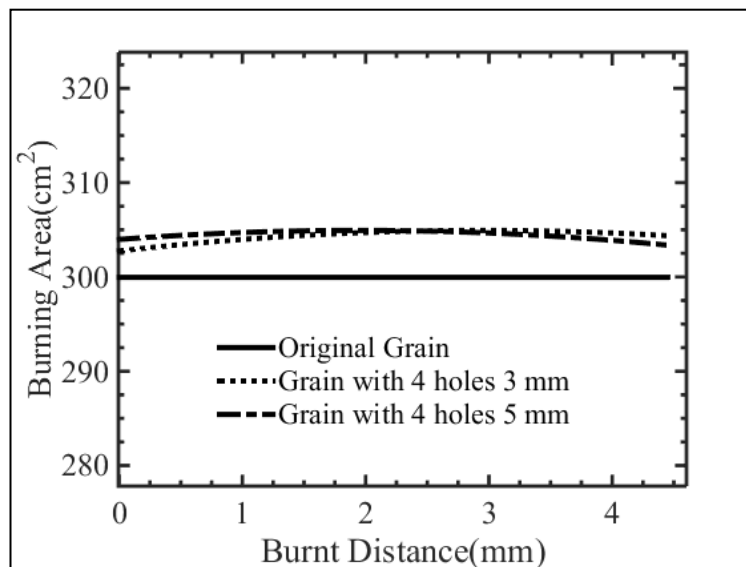


Figure 8. The changes of burning area without and with drilled holes.

Both time-averaged and high-frequency pressure measurements were taken at the motor head-end. The time-averaged measurements were made through one pressure port with one of HBM P3MB pressure strain-gauge transducer and one Kistler 6229A piezoelectric transducer covered with a thermal protective layer to record the high-frequency pressure oscillations. The test cases are described in table 2. In all of these tests, the pressure was measured at two positions, one was near to head and the other was near to nozzle, figure 9.



Figure 9. Test Stand.

5. Results

5.1. The P - t traces from the original motor and the modified motor

The static test results from the original motor are shown in figure 10 with the time-averaged pressure (in black) and the dynamic pressure (in green). It is clear that the pressure-time trace has no oscillations except at the ignition and burnout.

The modified motor shows a different pressure-time trace when statically fired, figure 11. First, a spectral analysis was done to investigate the frequency content of the original and the modified motor (it will be designated test #2). This analysis shows that there are exciting modes near 800 Hz and 1200 Hz, figure 12. The frequency for a given mode can be determined based upon chamber quantities of length, L , and the speed of sound inside a combustion chamber, a , as shown in equation (1)[2], where n is the mode number. The first longitudinal mode = 2165 Hz.

(1)

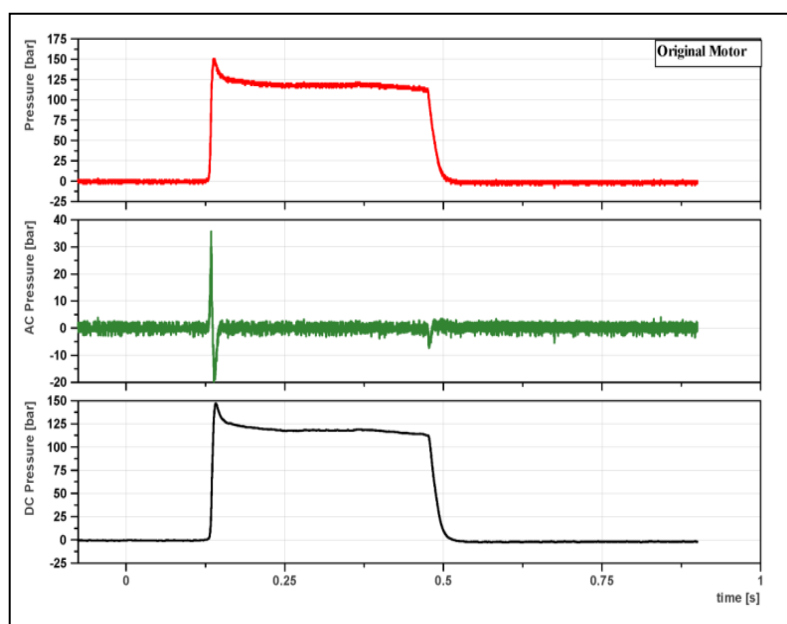


Figure 10. The (P - t) trace for original motor with multi-nozzle.

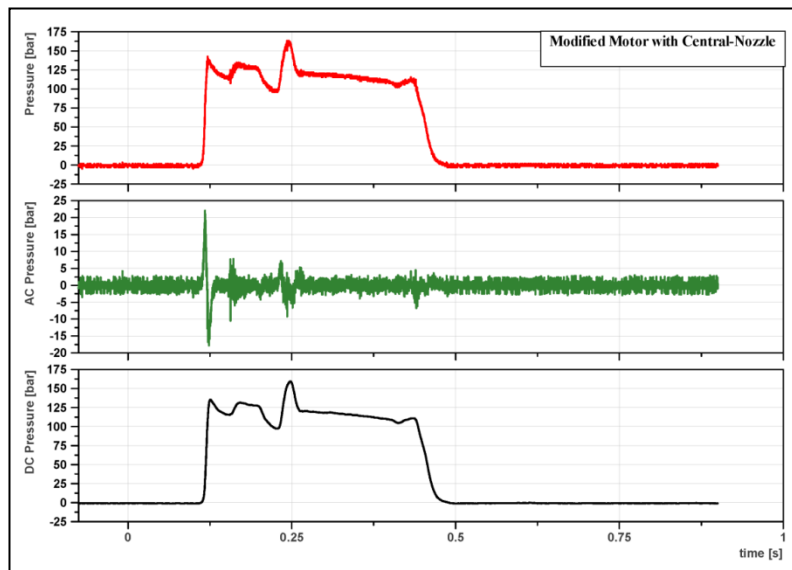


Figure 11.The (P-t) trace for modified motor with central-nozzle.

Figure 12, shows the power spectral density. It shows three broad peaks corresponding to the low-frequency instability. The bulk mode, and the first longitudinal mode are similar to those observed in a hybrid motor, figure 13[4]. It has been generally observed that the dominant mode involves low-frequency oscillations accompanied by lower amplitude higher frequency acoustic modes.

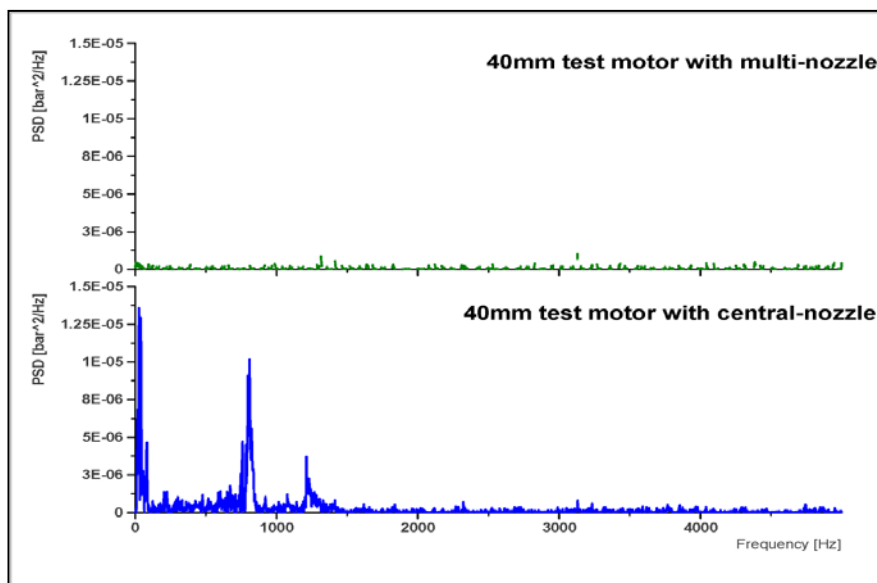


Figure 12. A spectral analysis performed for the two tests.

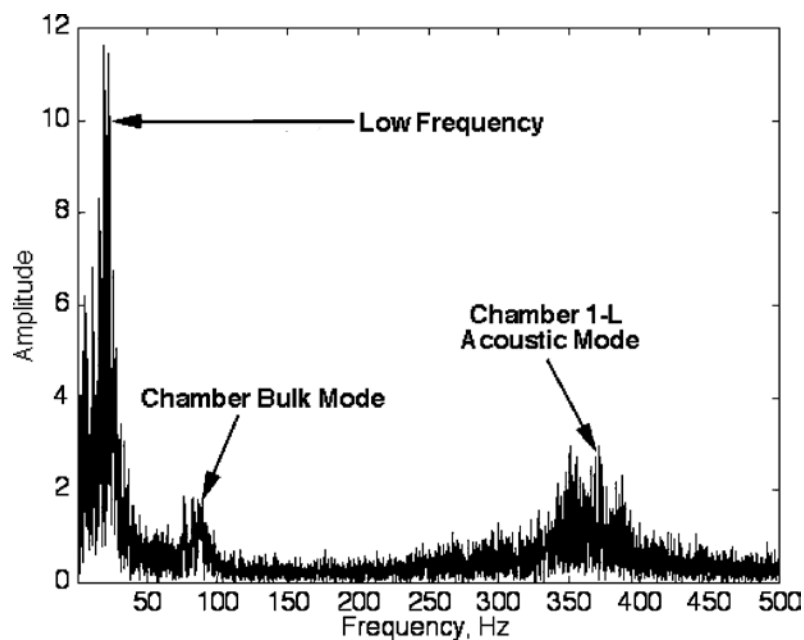


Figure 13. The Fourier transform corresponding to the low-frequency instability.

5.2. The *P-t* traces for the other cases.

Test #3 :(Resonance rod, central-nozzle dcr = 9.6 mm)

Resonance rods have been used to a much greater extent than any other device, the resonance rods were used to mitigate transverse modes of instability, with success. Resonance rods are installed in the grain perforation(s), either singly or in multiples, and are characterized by large length-to-width (transverse dimension) ratios but relatively small widths compared to the dimensions of the perforation. Various rod cross-sections have been used including rectangular, square, and circular cruciforms and shapes. Rods have been installed to extend either partially or over the full length of the grain perforation, and either cantilevered from one end or supported from both ends of the motor [22].

Resonance rod was applied successfully in control of instabilities in rocket motors MK40 and MK66 used in the American rocket Hydra (70 mm caliber), figure 14. For Talos cruise missile booster, figure 15, it is a good start to try to solve the problem of instability at expense of adding inert mass. In this case, the same resonance rod applied in MK66, figure 16, was tried. The *P-t* trace is shown in figure 17. The pressure spike at starting may be attributed to the decreased free volume inside the combustion chamber as the resonance rod is fitted inside the motor. The function of the resonance rod is to essentially disable the oscillations, meaning that the gas cavity is made acoustically random. However, this is often a difficult task since the mass of the rocket motor is required to be distributed symmetrically about the longitudinal axis. A common result of this requirement is that the suppressor, rather than creating randomness in the cavity, only "retunes" it. Another fundamental problem in the design of the mechanical suppressor is that the gas cavity is constantly changing, and the suppressor is often completely ineffective after the burn progressed partially, and this is what happened in this case as is evident from the figure.

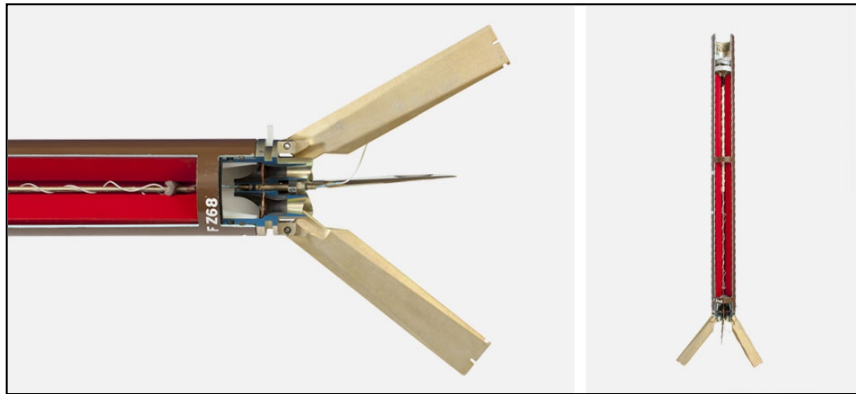


Figure 14. The American rocket Hydra (70 mm caliber)[23].

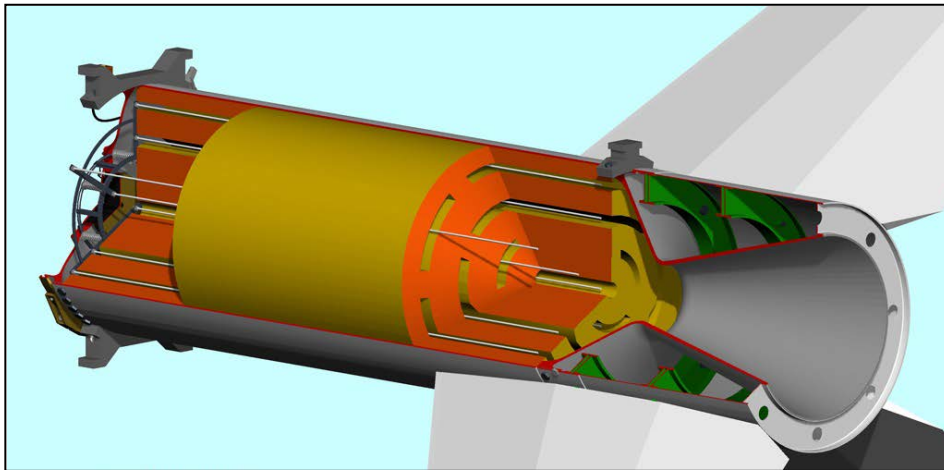


Figure 15. Talos cruise missile booster[24].



Figure 16. The resonance rod applied in MK66.

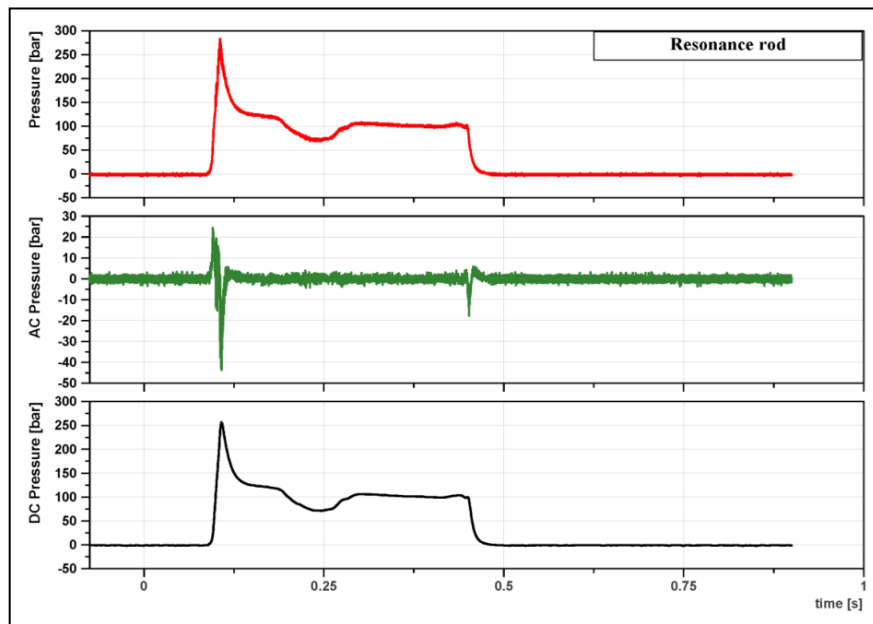


Figure 17.The modified motor tested with resonance rod (Test #3).

Test #4:(Grain with 3 holes radial, central-nozzle dcr = 9.6 mm)

Wimpress[15] has reported that by entirely empirical methods it has been found that several devices can be used to stabilize the burning in the central perforation, and the most common is the drilling of radial holes through the grain web at intervals along the axis. He reported also that two or more holes in a given plane at right angles to the axis of the grain have no more stabilizing effect than a single hole at the same point. The radial location of the holes is of no significance with respect to stabilizing effect, but it is general practice to avoid placing them in a single straight line because a radially unsymmetrical arrangement might affect the external ballistics of the rocket harmfully. In three-hole tubular grains, the radial holes are arranged in the form of a helix, with each hole in a plane passing through the axis of the grain but rotated 120° from the plane of the previous hole. Although it is apparent from figure 18, that irregularities gradually become less as the spacing between holes is decreased, it is not possible to establish definitely the maximum spacing compatible with stable burning.

The pressure-time curves obtained were more unstable than grain with three holes. Here, in this case, we confirmed that reducing the number of holes increases the problem of instability.

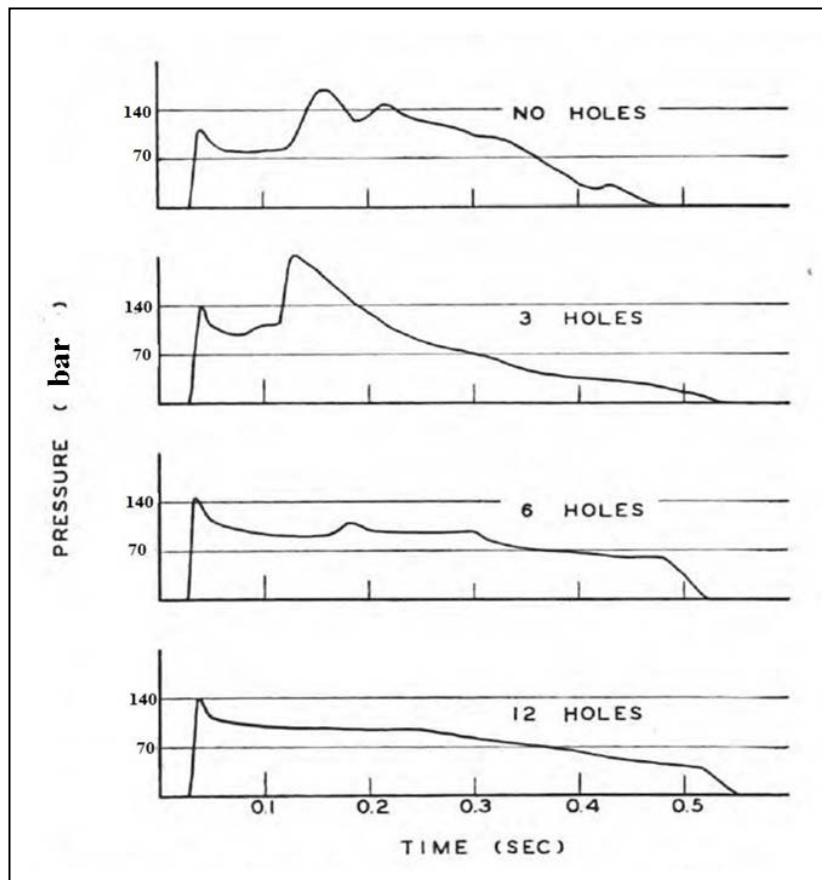


Figure 18. Stabilization of burning with radial holes taken from [14].

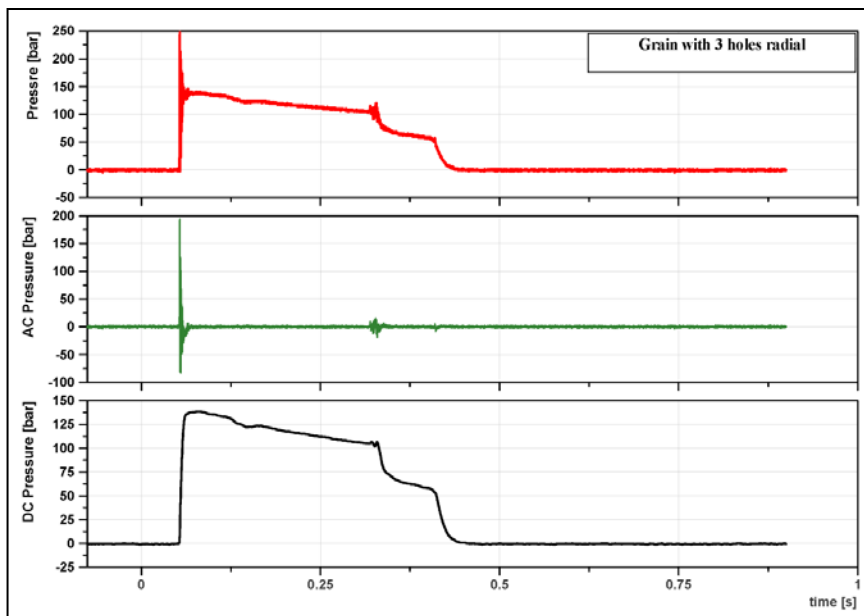


Figure 19. The modified motor tested with modified grain with 3 holes(Test #4).

Test #5 : (Grain with 2 holes radial, central-nozzle dcr = 9.6 mm)

The target of the holes was not achieved in this case, figure 20, as it appears that the number of holes was not sufficient to get rid of instability, but it was close to the target.

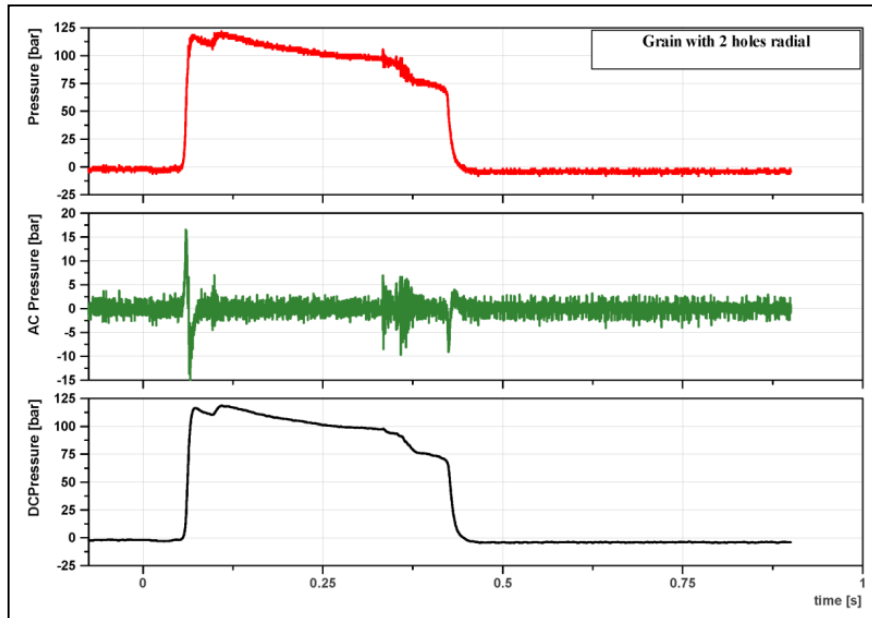


Figure 20. The modified motor tested with modified grain with 2 holes (Test #5).

Test #6:(Grain with 4 radial holes, central-nozzle dcr = 9.6 mm)

It seems that this is the most stable case. It is clear that the acoustic disturbances have decreased significantly, and this time the holes were effective in getting rid of the phenomenon of combustion instability, figure 21.

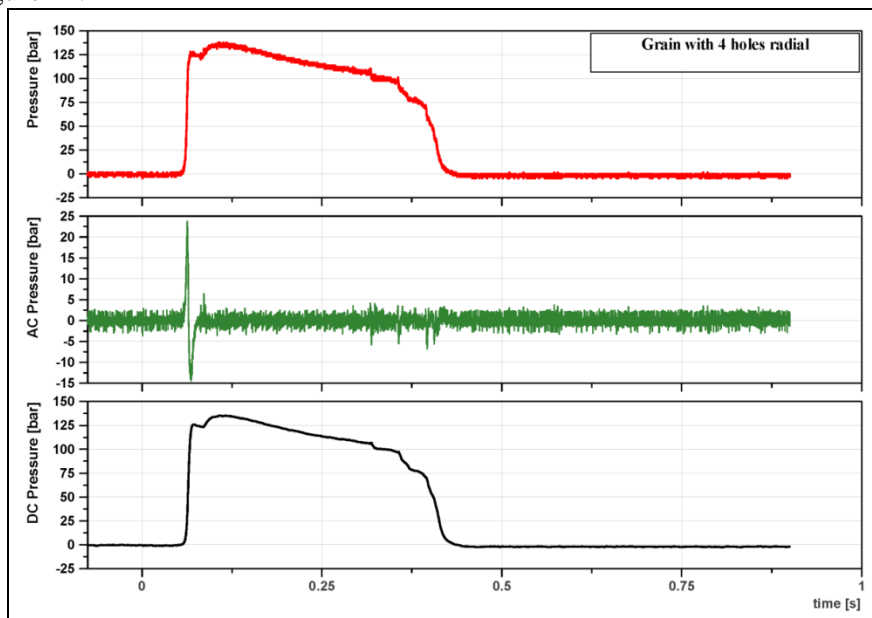


Figure 21. The modified motor tested with modified grain with 4 holes (test #6)

Test #7 :(Grain with 4 inline radial holes - Central-nozzle dcr = 9.6 mm)

The holes made on the same line were not as efficient as the other, which were not made on the same line, although the same distance between the holes was preserved, figure 22.

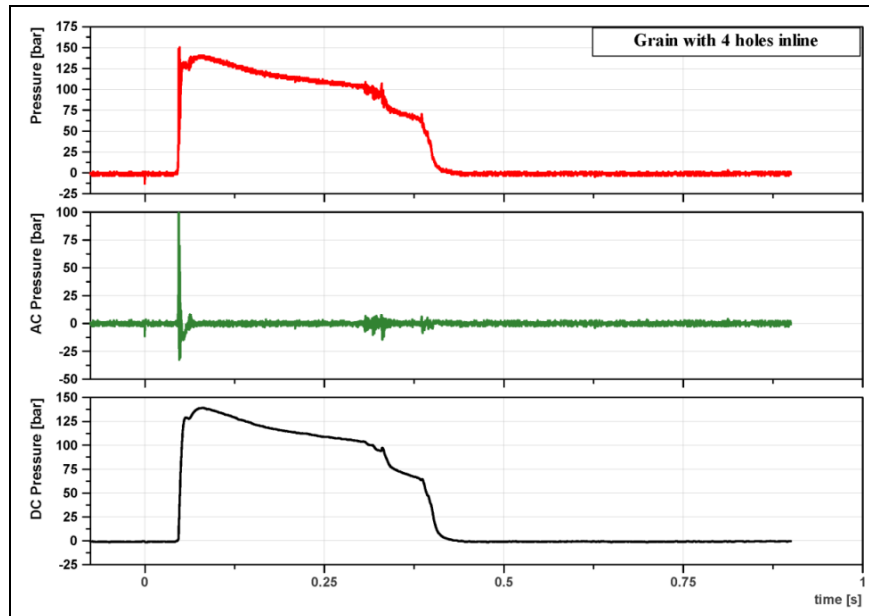


Figure 22. The modified motor tested with modified grain with 4 inline holes (Test #7).

Test #8:(Change blocking factor K_n , central-nozzle dcr = 10.6 mm)

The blocking factor K_n defined as ratio between burring area to throat area was reduced from 431 to 354, to test, The results showed that the problem has been worsened, figure 23

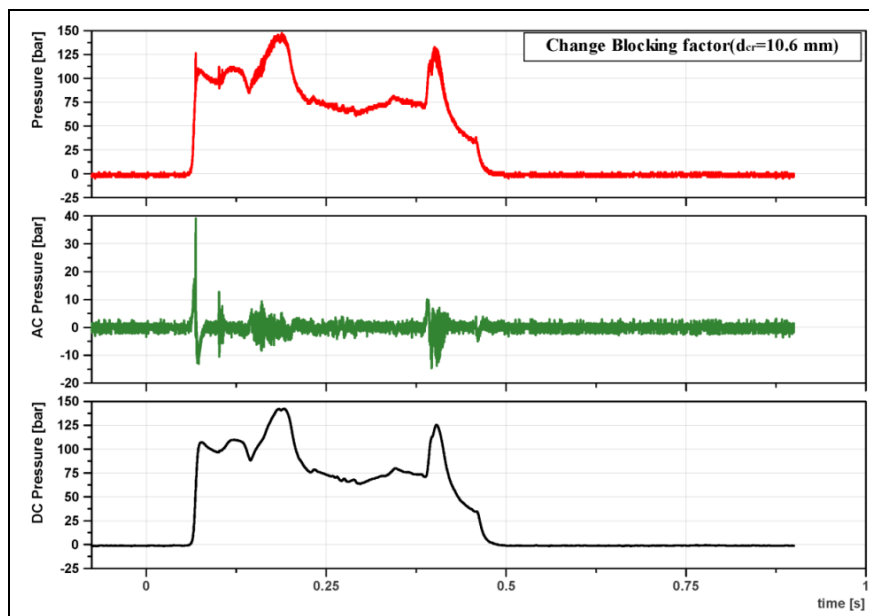


Figure 23. The modified motor tested with a throat diameter of 10.5 mm (Test #8).

Test #9:(Change blocking factor - central-nozzle $d_{cr} = 8.5$ mm)

The blocking factor was increased from 431 to 550, to mitigate combustion instability and it was positive. The effect of combustion instability was reduced, figure 24.

The results of the last two tests (increasing /decreasing blocking factor) show a decisive evidence for the phenomenon at hand to be an irregular burning rather than acoustic combustion instability. This is justified by referring to two researches.

According to Caprner et al. [25], they found that plotting the blocking factor K_n for both stable and unstable operations against combustion pressure, the intersection of the two plots being designated as the instability threshold, figure 25. From that figure, it is clear that the increasing pressure above the threshold pressure leads to instability, while from of Angelusetet al. [26] when he reported that the increasing pressure through increasing blocking factor leads to decrease irregular burning till all irregularities disappear, figure 26.

To summarize the results from these tests, all tests show irregular burning except for cases number 9 where the blocking factor was increased and case 6 of 4 drilled holes where the holes were not drilled on one line.

To have more investigation, a power spectral analysis was performed for the most stable case (test 6), figure 27. The curves show that even for such a stable case, there is still some acoustic or excited modes where there are relative peaks [26]. However, the powers contained in these peaks are too low to result in noticeable DC shifts as clear in other unstable cases.

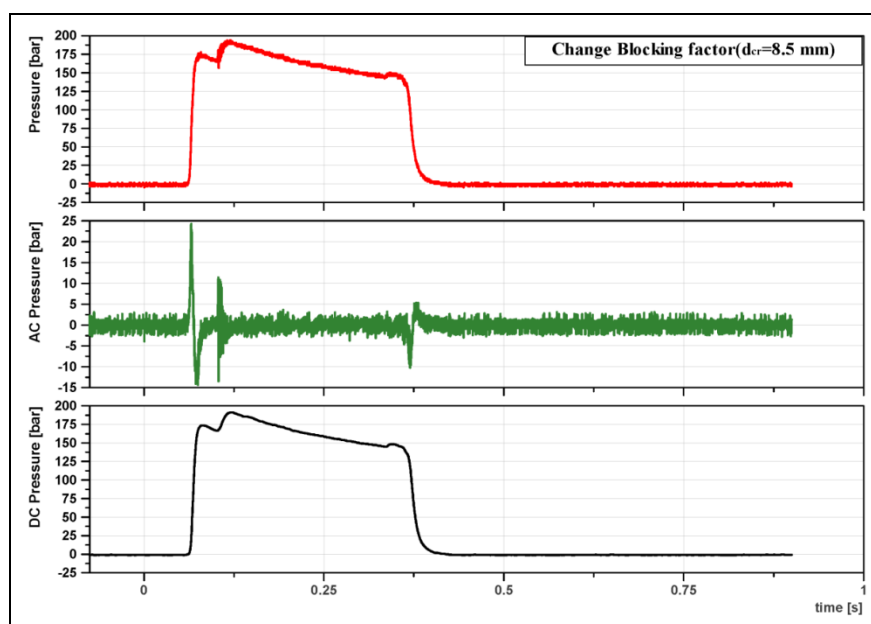


Figure 24. The modified motor tested with the throat diameter 8.6 mm (Test #9).

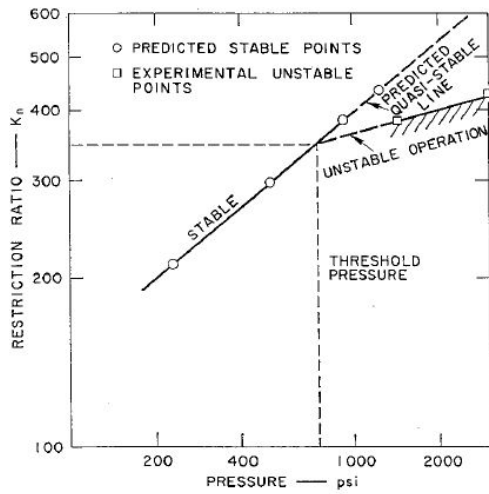


Figure 25. Selection of threshold point by extrapolating unstable data points back to K_n vs. P [25].

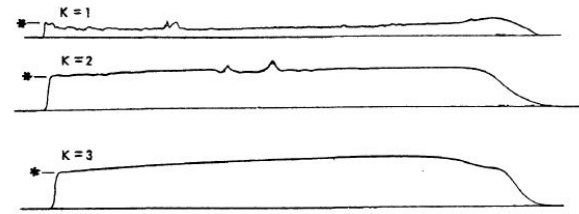


Figure 26. P-t traces for the same motor at different blocking factors, With increasing blocking factor, irregularities disappear.

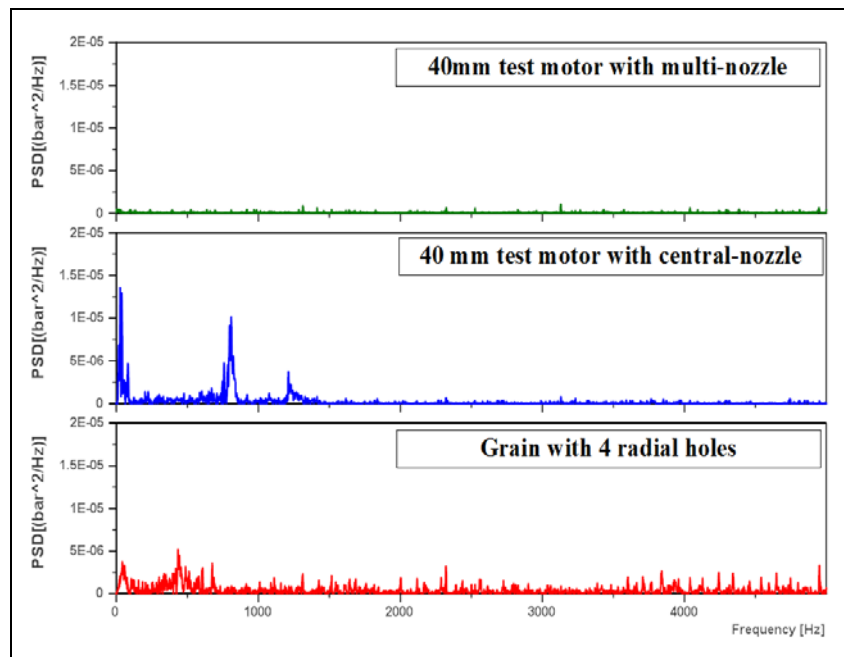


Figure 27. Power spectrum density.

The previous results are an experimental verification of the equation derived by Flandro[2]. It was shown that the change in time-average pressure is governed by the following equation (2)

$$\frac{d\bar{p}}{dt} = \left\{ \begin{array}{l} \left(\frac{\bar{\alpha}^2}{\gamma V}\right) (\bar{\rho} S_b (b\bar{P}^n) - \\ + \frac{\bar{\alpha}(\pi RL)}{2\gamma^2 V} \bar{P} \sum_{m=1}^{\infty} R_m^2 \{ \bar{M}_b (A_b^{(r)}) \} \end{array} \right. \quad (2)$$

where the classical first-order internal ballistics results are seen in the first term. S_b is the instantaneous burning surface area and A_{cr} is the nozzle throat area, C^* characteristic velocity. The standard model for the propellant burning rate is displayed with n as the burning rate exponent and \mathbf{b} as the coefficient. The second line shows the nonlinear correction indicating the effects of the pressure coupling where \bar{a} mean speed of sound, γ ratio of specific heats, \bar{P} mean chamber pressure, L chamber length, M_b Mach number in a combustion chamber, \mathbf{A}_b and \mathbf{B}_b are parameters of propellant admittance or pressure coupling terms, with $\mathbf{J}_m(\mathbf{k}_{mm})$ is the Bessel functions of order m , with summing over acoustic modes. It is obvious that large mean pressure shifts are expected when higher-order harmonics are excited in the nonlinear growth. It is important to understand that in this type of modeling effort, it is necessary to account for all internal ballistics effects including the changes of chamber volume and burning surface area with time as well as the modification of the surface Mach number as the average pressure rises. Form spectral analysis of unstable case (Test #2) and stable case (Test #6), the reason for the DC shift is clearly due to the excited modes at 800 and 1200 Hz, while in stable cases the amplitude of such waves (\mathbf{R}_m in equation 2) is very small, which results in too small time-averaged pressure[2].

Table 2. Summary of the test matrix

No.	Test name	Nozzle type	Irregular burning	
			Yes	No
1	Original motor 40 mm	Forward multi-nozzle		√
2	Modified motor 40 mm	Central-nozzle $d_{cr} = 9.6$ mm	√	
Mechanical Mitigation				
3	Resonance rod	Central-nozzle $d_{cr} = 9.6$ mm	√	
4	Grain with 2 holes radial	Central-nozzle $d_{cr} = 9.6$ mm	√	
5	Grain with 3 holes radial	Central-nozzle $d_{cr} = 9.6$ mm	√	
6	Grain with 4 holes radial	Central-nozzle $d_{cr} = 9.6$ mm		√
7	Grain with 4 holes inline	Central-nozzle $d_{cr} = 9.6$ mm	√	
Nozzle Damping				
8	Change blocking factor	Central-nozzle $d_{cr} = 10.6$ mm	√	
9	Change blocking factor	Central-nozzle $d_{cr} = 8.5$ mm		√

6. Conclusion

Combustion instability continues to hinder the development of solid propellant rocket motors from small motor such as the case discussed in this paper or for large motors used in the intercontinental ballistic missile. The problem with solving the combustion instability is that it cannot be extrapolated as the resonance rod which was applied successfully in a similar motor did not succeed in mitigating stability in this case.

Analysis of each case signal in time (time-averaged pressure and AC pressure) and frequency (Fourier transform amplitude and power spectral density) can explain how the instability happens. It was clear that exciting certain modes of chamber acoustic leads to instability. However, even for the stable cases, there are still some exciting modes but with a too-small amplitude that it cannot trigger instability or noticeable DC shift.

Despite that the general problem of acoustic instability had been studied for long times, the problem of irregular burning still needs more research in order to predict a priori the instability and predict the effectiveness of each fix to save the costs of experiments and labor works.

References

- [1] Blomshild F 2007 Lessons Learned In Solid Rocket Combustion Instability 43rd AIAA/ASME/SAE/ASEE Joint Propulsion Conference & Exhibit
- [2] FlandroG 2007 Irregular Burning: On the Origin of the DC Shift 43rd AIAA/ASME/SAE/ASEE Joint Propulsion Conference & Exhibit pp 1–17

- [3] *Engineering Design Handbook, Elements of Aircraft and Missile Propulsion*. AMCP.
- [4] Carmicino C and Pastrone D 2019 Acoustic Excitation as Triggering Mechanism of the 'DC Shift' Hybrid Rockets *AIAA J.* **57** no. 11, pp 4845–4853
- [5] Toong T, Richard F, John M, and Griffin Y 1965 Mechanisms of Combustion Instability *Proc. Combust. Inst.* **10** pp 1301-1313
- [6] Flandro G, Fischbach S, and Majdalani J 2007 Nonlinear rocket motor stability prediction: Limit amplitude, triggering, and mean pressure shift *Phys. Fluids* **19** no. 9
- [7] Flandro G, Perry E, and French J 2006 Nonlinear Rocket Motor Stability Computations: Understanding the Brownlee-Marble Observations *44th AIAA Aerospace Sciences Meeting and Exhibit*
- [8] Lengellé J, Duterque G., Trubert J 2002 Combustion of Solid Propellants (RTO-EN-023) *Intern. Aerodyn. Solid Rocket Propuls.* held Rhode-Saint-Genèse, Belgium, 27-31 May pp 27–31
- [9] Gusachenko Land. Zarko V 2008 Analysis of unsteady solid-propellant combustion models (review) *Combust. Explos. Shock Waves* **44** no. 1 pp 31–42
- [10] Green L 1956 Observations on the Irregular Reaction of Solid Propellant Charges *J. Jet Propuls.* **26** no. 8, pp 655–659
- [11] Gloyer P, Rice T, and Flandro G 2009 Ares i thrust oscillation mitigation via motor modifications *56th JANNAF Propulsion Meeting*
- [12] French J, Flandro G, Gloyer P, and Jacob E 2010 UCDS Nozzle Acoustic Dynamics and Stability Modeling *46th AIAA/ASME/SAE/ASEE Joint Propulsion Conference & Exhibit*
- [13] Larsen C, Gloyer P, and Flandro G 2008 Ares I Solid Rocket Booster Thrust Oscillation *NASA Eng. Saf. Cent. Tech. Report, RP-08-60*
- [14] Grad H 1949 Resonance burning in rocket motors *Commun. Pure Appl. Math.* **2** no. 1, pp 79–102
- [15] Wimpres R and Sage B 1950 Characteristics of burning in perforations *INTERNAL BALLISTICS OF SOLID-FUEL ROCKETS*, McGraw-Hill New York
- [16] Janardan B, Daniel B, and Zinn B 1974 Damping of Axial Instabilities by Small-Scale Nozzles Under Cold-Flow Conditions *J. Spacecr. Rockets* **11** no. 12 pp 812–820
- [17] Javed A and Chakraborty D 2014 Damping Coefficient Prediction of Solid Rocket Motor Nozzle Using Computational Fluid Dynamics *J. Propuls. Power* **30** no. 1 pp 19–23
- [18] ZINN B 1973 Nozzle Damping in Solid Rocket Instabilities *AIAA J.* **11** no. 11 pp 1492–1497
- [19] Sun B, Li S, Su W, Li J, and Wang N 2016 Effects of gas temperature on nozzle damping experiments on cold-flow rocket motors *Acta Astronaut.* **126** pp 18–26
- [20] Xing W, Wang N, Wei J, Dong Y, and Yan M 2013 Numerical Research on The Nozzle Damping Effect by A Wave Attenuation Method *Def. Technol.* **9** no. 3 pp 162–166
- [21] Janardan B and Zinn B 1977 Rocket nozzle damping characteristics measured using different experimental techniques *AIAA J.* **15** no. 3 pp 442–444
- [22] Oberg C, Haymes W, and Wong T 1972 Solid propellant combustion instability suppression devices *8th Joint Propulsion Specialist Conference*
- [23] FFAR Rocket System <https://fz.be/Mk40>
- [24] P. R. H. P. L. USNR-R <https://www.okieboat.com/Booster%20History.html>
- [25] Capener E, Dickinson L and Kier R 1964 Driving processes of finite-amplitude axial mode instability in solid-propellant rockets *AIAA J.* **5** no. 5 pp 938–945
- [26] Angelus T 1960 Unstable Burning Phenomenon Double-Base Propellants *Solid Propellant Rocket Research*, New York: American Institute of Aeronautics and Astronautics pp 527–559.